Journal of Renewable Materials

Tech Science Press

Bio-Based Hyperbranched Toughener From Tannic Acid and Its Enhanced Solvent-Free Epoxy Resin with High Performance

Jie Xu[1,3], Jiayao Yang[1], Hengxu Wang[1], Peng Lin[2], Xiaohuan Liu[1,*], Jinjie Zhang[1], Shenyuan Fu[1,*] and Yuxun Tang[2,*]

[1]School of Engineering, and Zhejiang Provincial Collaborative Innovation Center for Bamboo Resources and High-Efficiency Utilization, Zhejiang A & F University, Hangzhou, 311300, China.

[2]Zhonghang Monitoring Technology Research Institute Co., Ltd., Hangzhou, 310022, China.

[3]Zhejiang Runyang New Material Technology Co., Ltd., Huzhou, 313105, China.

[*]Corresponding Authors: Xiaohuan Liu. Email: liuxiaohuancaf@163.com; Shenyuan Fu. Email: fshenyuan@sina.com; Yuxun Tang. Email: yxtom@sina.com.

Abstract: It is essential to design economic and efficient tougheners to prepare high-performance epoxy resin; however, this has remained a huge challenge. Herein, an eco-friendly, low-cost, and facile-fabricated bio-based hyperbranched toughener, carboxylic acid-functionalized tannic acid (CATA), was successfully prepared and applicated to the preparation of solvent-free epoxy resins. The mechanical performance, morphology, structural characterization, and thermal characterization of toughened epoxy resin system were studied. The toughened epoxy resin system with only 1.0wt% CATA reached the highest impact strength, 111% higher than the neat epoxy resin system. Notably, the tensile strength and elongation at break of toughened epoxy resin systems increased moderately with increasing CATA loading. Nonphase-separated hybrids with significant toughening effect were obtained. Additionally, the thermal stabilities of toughened epoxy resin systems decreased with increasing CATA loading. This study provides an eco-friendly, cost-effective, and facile approach for the preparation of high-performance, solvent-free epoxy resins with potential for practical applications in sealing integrated circuits and electrical devices fields.

Keywords: Solvent-free epoxy resins; bio-based toughener; bio-based curing agent; mechanical performance; thermal properties

1 Introduction

Epoxy resins are one of the major classes of thermosets with an estimated market value of $33.6 billion in 2022. Owing to their excellent mechanical strength, thermal stability, and chemical resistance, they have wide applications in several areas including adhesives, coatings, and, structural composites [1-3]. Solvent-free epoxy resin is a new type of epoxy resin without any solvent. Solvent-free epoxy resins offer significant merits including the following: free of volatile organic compounds (VOCs), nontoxicity, good processability, high recycling rate, energy saving, and ease of use [4,5]. Compared to conventional liquid epoxy resin, the curing of solvent-free epoxy resin is different because it occurs in the molten phase. Melting, flow, gel point, and cure completions are the principal stages in solvent-free epoxy resins [6]. Additionally, solvent-free epoxy resins do not contain a variety of VOCs such as hydrocarbons, ketones, alcohols, and esters [7]. Solvent-free epoxy resins based on epoxy resins have shown several advantages, including outstanding mechanical properties, good processability, and thermal resistance [8,9]. However, the high crosslinking density of epoxy resins leads to inadequate toughness, thus limiting its use in applications requiring good impact strength [10]. Various materials such as clay [11], rubber, nanomaterial [12,13], hyperbranched polymers [11], and engineering plastic particles have been

introduced into epoxy materials to improve mechanical properties, especially impact strength and tensile strength [2]. But the key point for these methods is to toughen epoxy resin without sacrificing mechanical strength and thermal properties [2].

With diminishing petroleum oil reserves and severe environmental pollution [14,15], material scientists are increasingly interested in using bio-based renewable resources to prepare bio-based products. Bio-based renewable feedstocks such as lignin [16-22], cellulose [23,24], rosin [25], catechin [26], plant oil [27-29], sucrose [30], itaconic acid [31], tannic acid, and many other naturally derived materials have attracted much attention in various industrial applications [32]. For instance, tannic acid (TA) is a naturally available nonhazardous polyphenolic compound containing abundant terminal phenol hydroxyl groups [33-37]. Fei et al. [2] synthesized carboxylic acid-functionalized TA (CATA) from TA and methylhexahydrophthalic anhydride (MeHHPA); CATA improved the toughness of epoxy resins. In addition, Liu et al. [38-40] synthesized maleopimaric acid (MPA) via the Diels-Alder reaction of rosin acid with maleic anhydride; MPA was used as a bio-based curing agent for epoxy resin. In all these studies, MPA and the CATA were used to modify the formulations of solvent-based epoxy resins. At present, these studies provide no information about MPA and CATA in the formulation of solvent-free epoxy resins. Therefore, it is not clear whether incorporation of MPA and CATA into solvent-free epoxy resins can improve the mechanical and thermal properties.

The aim of this study is to investigate whether covalent incorporation of CATA into solvent-free epoxy resins can improve the toughness and thermal properties. Herein, the structure, curing behavior, mechanical performance, and thermal properties of toughened epoxy resin systems were investigated. The study demonstrates the facile fabrication of solvent-free epoxy resins with high strength, high heat resistance, and high toughness via the incorporation of epoxy resin (E-12), MPA, 2-methyl imidazole (2-MI), and CATA (Scheme 1). This study offers a novel strategy for the design of integrated strong and tough solvent-free epoxy resins.

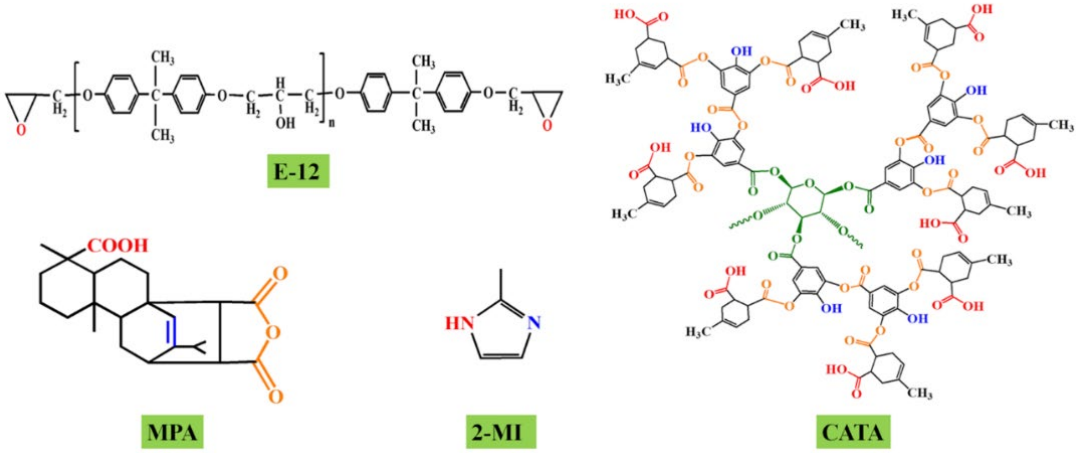

Scheme 1: Chemical structures of E-12, MPA, 2-MI, and CATA

2 Experimental

2.1 Material

TA (TA, $C_{76}H_{52}O_{46}$), abietic acid (AA, $C_{20}H_{30}O_2$), maleic anhydride (95%), *p*-toluene sulfonic acid, 2-MI ($C_4H_6N_2$), pyridine, sodium hydroxide, and organic solvents were obtained from Sino pharm Chemical Reagent Co., Ltd. (Shanghai, China). E-12 was supplied by Huangshan Jinfeng Industrial Co., Ltd. (Anhui, China). MeHHPA (molecular formula $C_9H_{12}O_3$, molecular weight: 168.19 g/mol) was purchased from Linan Carl Biological Technology Co., Ltd. (Hangzhou, China).

2.2 Synthesis of MPA

AA (30 g) was added to a three-necked 250-mL flask. The flask was transferred to a 160°C oil bath and stirred for 2 hunder N_2 atmosphere to yield levopimaric acid. The reaction was cooled to 110°C, and then100 mL acetic acid, 7.1 g maleic anhydride, and 1.6 g *p*-toluene sulfonic acid were added into the above reaction. The obtained mixture was then refluxed at 110°C for another 5 h; the mixture was subsequently cooled to 30°C. A yellow solid product was obtained; it was washed with acetic acid several times. Finally, a white crystal product of MPA was obtained after drying under vacuum (yield: 90%) (Scheme 2) [38].

2.3 Synthesis of CATA

CATA was synthesized using a one-pot $A_2 + B_3$ approach. Under N_2 protection, TA (5 g), pyridine (50 mL), and MeHHPA (23 mL) were added to a three-necked 100-mL flask and mixed under vigorous stirring at 30°C for 10 min. The above solution was kept at 90°C and lasted for 48 h. After removing the pyridine and unreacted MeHHPA, the resulting product was precipitated with diethyl ether. The obtained product was dissolved in 50 mL tetrahydrofuran and subsequently poured into 100 mL deionized water. Finally, a precipitate was collected via filtration and dried at 40°C in an oven for 12 h. A solid brown product of CATA was obtained with a yield of 92% (Scheme 2) [2].

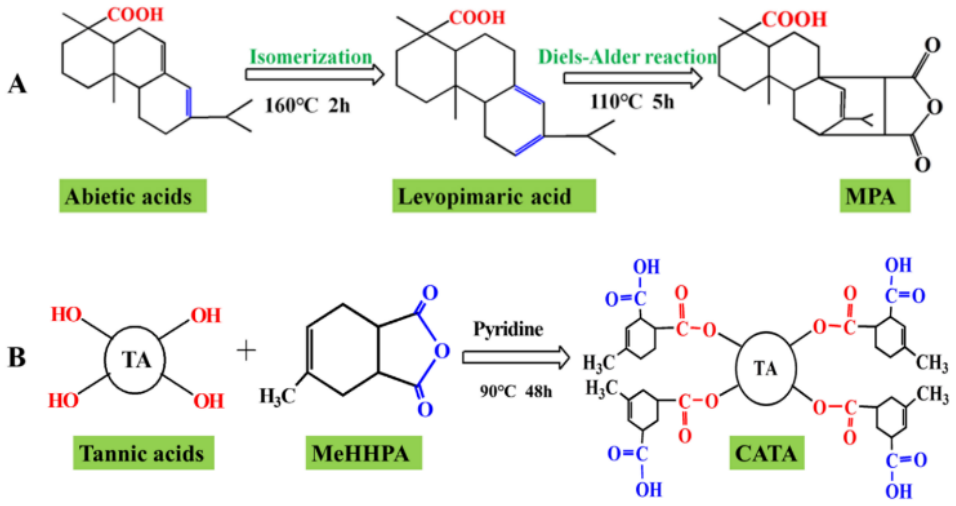

Scheme 2: Synthesis route of (A) MPA and (B) CATA

2.4 Preparation of Cured Epoxy Samples

A mixture of E-12 and MPA in a 1:0.8 equivalent ratio without solvent was heated and kept at 100°C for 10 min until the mixture reached the molten state. The molten blends were rapidly cooled and hardened into solid and ground into a solid. Then, catalyst (2-MI, 1.0 wt% of the total weight) and a desired amount of CATA were introduced to form a homogenous mixture (the final curing system). The as-prepared CATA-reinforced E-12/MPA/2-MI systems were transferred into a preheated metal mold and preheated at 150°C for 5 min followed by pressing at 8MPa for 60 min followed by cool pressing for 5 min. Finally, the samples of E-12/MPA/2-MI/CATA systems were shaped into the desired size for further measurements. All the samples were cured under the same conditions. The solvent-free epoxy resins were named as Neat, CATA 0.25, CATA 0.5, CATA 1, CATA 2, and CATA 3 (Tab. 1). The nomination is based on different CATA loadings in the solvent-free epoxy resins. “Neat” stands for the E-12/MPA/2-MI system without any CATA addition.

Table 1: Composition and ratio of CATA-reinforced epoxy resin systems

Sample No.	E-12 (wt%)	MPA (wt%)	2-MI (wt%)	CATA (wt%)
Neat	91.6	7.4	1	0
CATA 0.25	91.4	7.35	1	0.25
CATA 0.5	91.2	7.3	1	0.5
CATA 1	90.7	7.3	1	1
CATA 2	89.8	7.2	1	2
CATA 3	88.9	7.1	1	3

2.5 Characterization

FTIR spectra were recorded using a Perkin Elmer 1100 spectrophotometer using KBrpellets at room temperature in the mid-infrared region (4000-500 cm^{-1}). ^{1}H-NMR and ^{13}C-NMR spectra were recorded using a Bruker AVANCE 400 NMR spectrometer using $CDCl_3$ as the solvent. DSC measurements were carried out using a Netzsch STA 409PC Maia instrument in a N_2 gas stream (50 mL/min purge flow). Dynamic mechanical analysis (DMA)was performed using a Q800 TA instrument. The tests were performed with a heating rate of 3 °C/min from 60°C to 220°C and a frequency of 1 Hz under air atmosphere. The sample was mounted on a single cantilever clip. Un-notched impact strength experiments were conducted using a pendulum impact testing machine according to ISO 179:1982 standard. Each sample measuring 80 mm × 10 mm × 4 mm was used for this evaluation. The tensile strength of samples was characterized using an electronic universal testing machine according to ISO 527:1993 standard. SEM micrographs were obtained using a TM3030 field-emission scanning electron microscope at an accelerating voltage of 15000 V. TGA experiments were performed using an STA 409PC instrument with high-purity N_2asthe purge gas at a scanning rate of 20 °C/min from 40°C to 800°C. Samples of ~ 5 mg initial weight were kept in an open Pt pan.

3 Results and Discussion

3.1 Mechanical Performance

To evaluate the loading level of CATA on the mechanical properties of as-prepared CATA-reinforced epoxy resin systems, the impact strength, elongation at break, modulus, and tensile strength were measured. The results are shown in Fig. 1. As shown in Figs. 1(A), 1(C), and 1(D), clearly a small amount of CATA uniformly dispersed in E-12/MPA/2-MI systems simultaneously increased the tensile properties and impact strength. The impact strength of CATA 1 significantly increased and then decreased at higher loadings. Interestingly, addition of only 1.0 wt% CATA-reinforced epoxy resin system led to a 111% increase in the impact strength (from 7.9 KJ/m^2 to 16.7 KJ/m^2). In addition, Fig. 1(B) shows typical stress-strain curves of CATA-reinforced epoxy resin systems. The tensile strength of CATA-reinforced epoxy resin systems increased with increasing CATA loading.

In typical epoxy materials, an increase in tensile strength could lead to a decrease in elongation at break owing to mutually exclusive mechanical mechanisms between tensile strength and toughness [41]. However, the elongation at break and tensile strength of CATA-reinforced epoxy resin systems increased with increasing CATA loading from 0 to 3.0 wt%. Compared with neat epoxy system, the tensile strength, modulus, and elongation at break of CATA3 improved by ~ 42.5% (up to 50.6 MPa), 8.4% (up to 1045 MPa), and 35.9% (up to 4.43%), respectively. Such an increase can be explained by the formation of good interface interaction and introduction of a rigid aromatic structure in the curing system.

Based on the above mechanical analysis, a reasonable conclusion can be drawn. The increase in fractional free volume is beneficial to the increase in impact strength and elongation at break [42], whereas rigid aromatic structures could be used to explain the increase in tensile strength. CATA 1 showed a high toughness of 16.7 KJ/m^2, a tensile strength of as high as 47.8 MPa (the ultimate value up to 50.6 MPa), and a modulus as high as 1052 MPa (the ultimate value up to 1076 MPa).

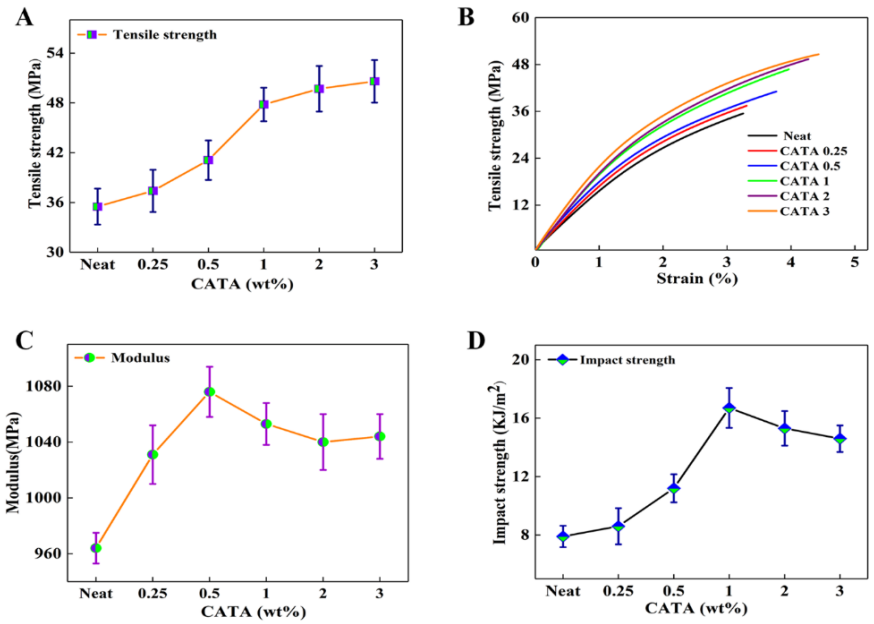

Figure 1: (A) Tensile strength of CATA-reinforced epoxy resin systems with different CATA loadings; (B) typical stress-strain curves of CATA-reinforced epoxy resin systems with different CATA loadings; (C) modulus and (D) impact strength of CATA-reinforced epoxy resin systems with different CATA loadings

3.2 Morphology

The impact fracture surface morphology of CATA-reinforced epoxy resin systems was also visually analyzed by SEM to better understand the mechanical reinforcement effect of CATA. As shown in Figs. 2(A)-2(F), the fracture surface of cured neat epoxy system is relatively smooth and flat except for some river-like lines, typical for a brittle failure [33,43]. In contrast, the fracture surface of cured CATA 1is rougher than that of neat epoxy system and shows signs of fibrils formation. Many oriented "fibrils" involves significant energy-absorbing processes. As CATA was added into the epoxy resin system, the quantity of "fibrils" increase [44], especially CATA 1 (Fig. 2(D)), thus improving the toughness of CATA-reinforced epoxy resin systems. In addition, cavities and particles were not observed in the fracture surface morphology, indicating that CATA-reinforced epoxy resin systems have no trace of phase separation. This result can be attributed to the participation of CATA in the crosslinking network, forming a homogenous system after curing. CATA-reinforced epoxy resin systems improved toughness by increasing the free volume and deformation of cavities, consistent with *in-situ* toughening mechanism [45].

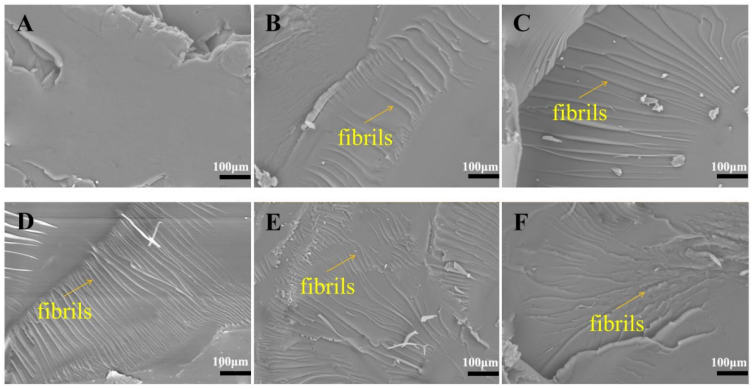

Figure 2: SEM micrographs of fracture surfaces of impact samples: (A) Neat, (B) CATA 0.25, (C) CATA 0.5, (D) CATA 1, (E) CATA 2, and (F) CATA 3

3.3 Structural Characterization

The chemical structures of AA, MPA, CATA, and TA were characterized by FT-IR, ^{1}H-NMR, and ^{13}C-NMR spectroscopy. In the FTIR spectra (Fig. 3), for pristine AA, the peak at 1707 cm^{-1} is assigned to carbonyl stretching vibration band. Compared with unmodified AA, MPA shows the C-O-C bands at 1084 cm^{-1} and the peaks appeared at 1778 cm^{-1}, 1837 cm^{-1} (C=O of anhydride), indicating the existence of carbonyl carbons after modification. The results show that MPA was successfully synthesized by the Diels-Alder reaction of maleic anhydride with levopimaric [38-40]. Moreover, CATA shows a decrease in the absorption intensity of OH region (3400 cm^{-1}); three new distinct peaks appeared at 2952 cm^{-1}, 2856 cm^{-1} (C-H of MeHHPA), and 1734 cm^{-1} (C=O of ester), indicating that CATA was successfully synthesized.

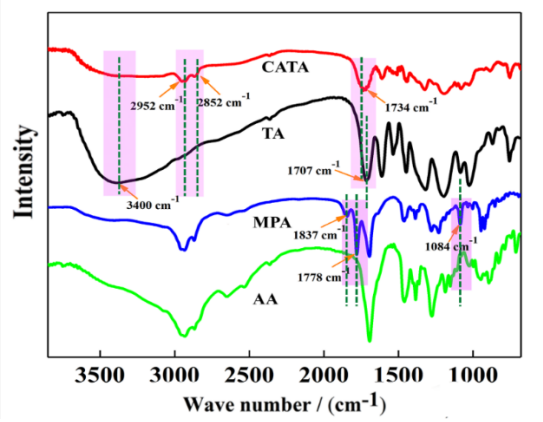

Figure 3: FTIR spectra of CATA, TA, MPA, and AA

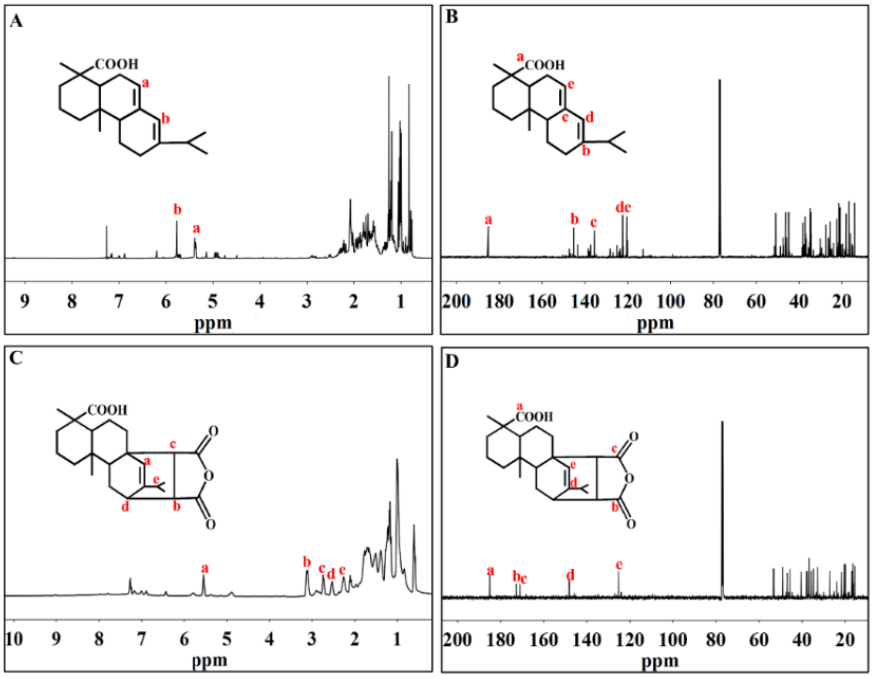

Figure 4: ^{1}H-NMR spectra of (A) AA and (C) MPA and ^{13}C-NMR spectra of (B) AA and (D) MPA

NMR is a powerful tool to characterize the chemical structure of samples. As shown in the ^{1}H-NMR and ^{13}C-NMR spectra of AA, MPA, TA, and CATA (Figs. 4 and 5), the^{1}H-NMR spectrum of MPA and the corresponding proton assignments are shown in Fig. 4(C). In the spectrum of MPA, the peak at 5.5 ppm can be assigned to proton H_a on the unsaturated carbon. In addition, other series of characteristic

peaks at 3.1 ppm (proton H_b), 2.7 ppm (proton H_c), 2.5 ppm (proton H_d), and 2.2 ppm (proton H_e) were also observed. The ^{13}C-NMR spectrum of MPA and the corresponding proton assignments are shown in Fig. 4. The main difference observed between the ^{13}C-NMRspectra of AA (Fig. 4(B)) and MPA (Fig. 4(D)) is the presence of carbonyl carbons from the grafted anhydride group located at 171.5 ppm and 173.4 ppm. The ^{1}H-NMR and ^{13}C-NMR results of MPA are consistent with the result of rosin acid reported by Liu et al. [38].

Fig. 5 shows the ^{1}H-NMR and ^{13}C-NMR spectra of TA and CATA. Fig. 5(C) shows the ^{1}H-NMR spectrum of CATA and the corresponding proton assignments. The peaks at 1.7, 5.5, and 12.3 ppm can be assigned to the protons in CH_3-C=C-, -CH=CH-, and -COOH groups, respectively. Similarly, the ^{13}C-NMR spectrum of CATA is shown in Fig. 5(D). The peak at 176.3 ppm was assigned to the -COOH groups. The characteristic peaks for the aliphatic carbons from MeHHPA appeared at 25.1 ppm, 28.6 ppm, 32.7 ppm, 42.5 ppm, 123.2 ppm, and 136.4 ppm. The ^{1}H-NMR and ^{13}C-NMR results indicate that CATA was successfully prepared, consistent with the literature [2]. By combining the results obtained from FT-IR, ^{1}H-NMR, and ^{13}C-NMR, the chemical structures of MPA and CATA were further confirmed; they are consistent with the predicted structures.

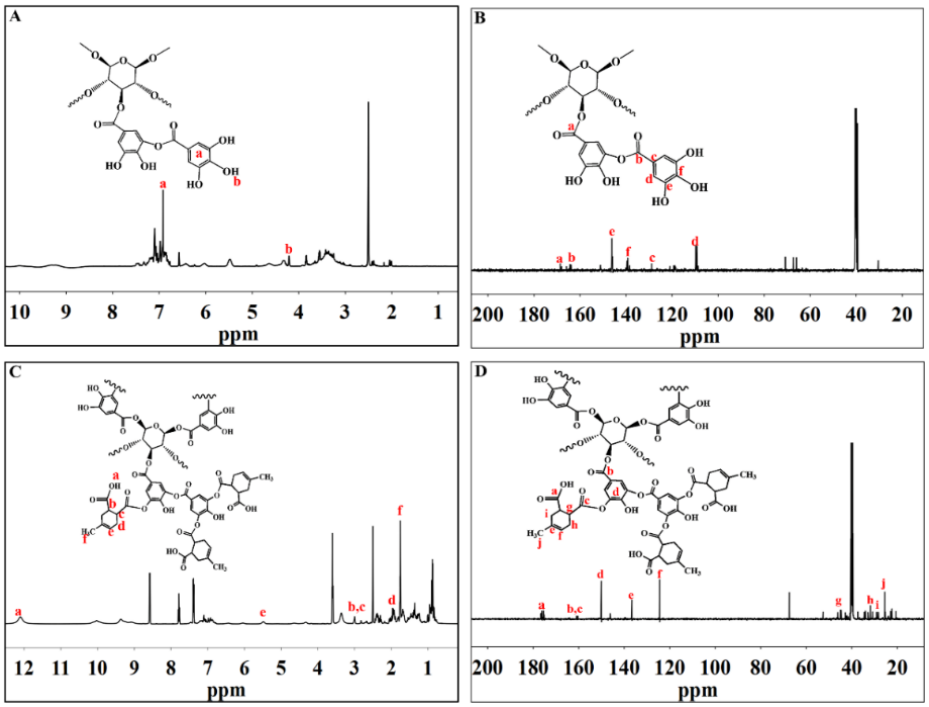

Figure 5: ^{1}H-NMR spectra of (A) TA and (C) CATA and ^{13}C-NMR spectra of (B) TA and (D) CATA

3.4 Thermal Characterizations

3.4.1 DSC Analysis

Nonisothermal curing behaviors of the CATA-reinforced epoxy resin systems were evaluated by DSC. The DSC traces of CATA-reinforced epoxy resin systems and neat epoxy system with the results are shown in Tab. 2 and Fig. 6(A). With the introduction of CATA into the epoxy resin system, the curing temperature of CATA-reinforced epoxy resin systems became significantly lower than that of neat epoxy system. The peak temperatures shifted toward lower temperatures with increasing CATA loadings. This is probably because the increase in CATA loading accelerated the curing reaction of epoxy resin system.

Table 2: DSC and TGA results of CATA-reinforced epoxy resin systems with different CATA loadings

Sample	T_i(°C) [a]	T_p(°C) [a]	$T_{5\%}$ (°C) [b]	$T_{50\%}$(°C) [b]
Neat	96.7	175.4	361.5	467.9
CATA 0.25	92.4	166.1	350.8	463.5
CATA 0.5	85.2	159.6	334.7	458.4
CATA 1	80.5	153.7	295.4	456.6
CATA 2	77.3	145.8	283.5	451.3
CATA 3	72.8	141.3	274.6	447.6

[a]T_i and T_p are the initial temperature and peak temperature obtained from differential scanning calorimetry, respectively; [b]$T_{5\%}$ and $T_{50\%}$ are the temperature corresponding to 5% weight loss and 50% weight loss, respectively, as obtained from thermogravimetric analysis.

Further, various curing degrees (α) were evaluated by measuring the total area (dH_T) under the DSC curve and partial area (dH) at a definite temperature. Degree of curing (α) is the ratio of dH to dH_T [42]. The curve of conversion *vs.* temperature as a function of CATA concentration also shows a similar result in Fig. 6(B). A significant increase in the conversion of CATA-reinforced epoxy resin systems at a given temperature was observed as the loading of CATA increased.

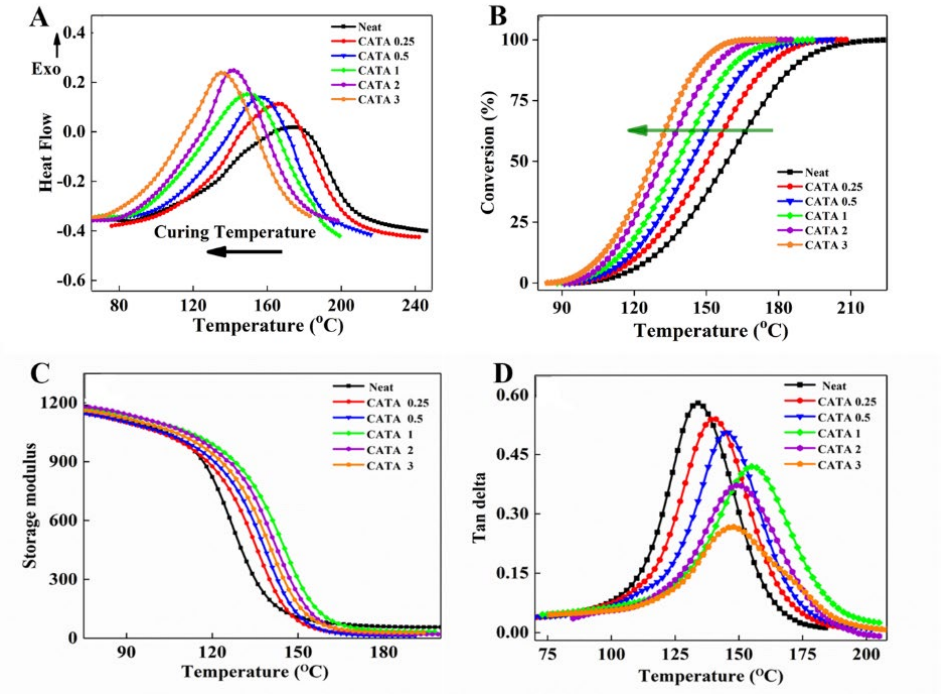

Figure 6: (A) DSC thermograms of CATA-reinforced epoxy resin systems with different CATA loadings; (B) conversion *vs.* temperature at different CATA loadings. CATA loadings increase along the direction of arrow; (C) storage moduli and (D) tan delta *vs.* temperature for the CATA-reinforced epoxy resin systems with different CATA loadings

These results indicate that CATA introduced into the epoxy resin system clearly accelerated the curing. The acceleration effect can be explained as follows: On one hand, CATA contained a large amount of terminal carboxyl groups [10] that served as a curing agent and reacted with the epoxy group at a low temperature. On the other hand, a small amount of unreacted hydroxyl groups [46] activated the anhydride groups and significantly enhanced the reactivity between the anhydride groups and epoxy groups.

CATA-reinforced epoxy resin systems have a complex curing reaction mechanism. The terminal carboxyl groups on CATA react with the epoxy group, opening the epoxy ring and producing hydroxyl groups and ester units that subsequently reacted with MPA, forming new carboxyl groups and ester units (Scheme 3).

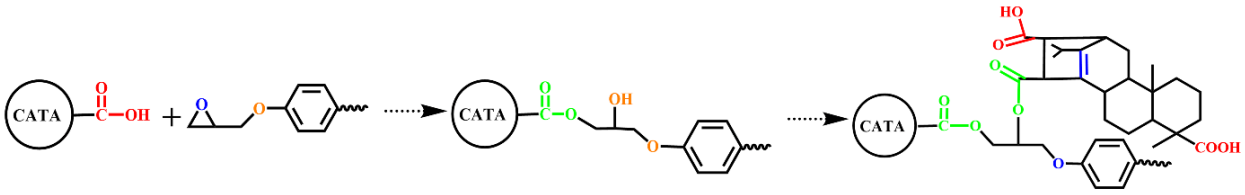

Scheme 3: Effect of CATA on the curing of epoxy resin system

3.4.2 DMA Analysis

The storage moduli (E') and loss tangent ($Tan\ \delta$) as a function of temperature for neat epoxy system and CATA-reinforced epoxy resin systems are shown in Figs. 6(C) and 6(D) (DMA analysis), respectively. Each curve of all systems shows a good rubbery plateau modulus (E_r) and a clear glass transition. Clearly, each composition exhibited a drastic decrease in E' and one corresponding peak during the transition from a glassy state to rubbery state, indicating no sign of phase separation during mixing and curing. With increasing temperature, the moduli reached the elastomeric region through the glass transition region, where many segments in the chains moved in a cooperative manner [47]. As shown in Fig. 6(C), compared with neat epoxy system, the rubbery plateau modulus (E_r) experiment data of CATA-reinforced epoxy resin systems indicate that E_r decreased with the incorporation of CATA. This is probably because the larger steric hindrance and possibility of chain back folding led to a lower crosslinking density. According to classical rubber elasticity, E_r is proportional to the crosslinking density [10,48].The crosslinking density (ρ) can be expressed as follows:

$$\rho = \frac{E_r}{3RT} \tag{1}$$

where ρ, E_r, and T are the crosslinking density per unit volume (mol/cm^3), rubbery plateau modulus, and absolute temperature at $T_g + 30$°C, respectively [33,49].

Table 3: DMA results of neat system and CATA-reinforced epoxy resin system with different CATA loadings

Sample	T_g(℃)	Storage modulus (MPa)		ρ (10^{-3} mol/cm^3)
		glassy region[a]	rubbery region[b]	
Neat	134.5	1258	31.2	2.86
CATA 0.25	140.7	1205	25.4	2.46
CATA 0.5	145.2	1194	24.7	2.37
CATA 1	159.7	1224	25.1	2.32
CATA 2	152.1	1231	23.6	2.23
CATA 3	149.2	1215	23.1	2.19

[a] Storage modulus at 70°C; [b] Storage modulus at $T_g + 30$°C.

Theoretically, the trends are the same: The crosslinking density (ρ) decreased with decreasing E_r. Unexpectedly, the crosslinking density of CATA-reinforced epoxy resin systems is lower than neat epoxy system. Moreover, the crosslinking density of CATA-reinforced epoxy resin systems decreased with increasing CATA loadings. This can be explained as follows: On one hand, the steric hindrance of TA

restrained the curing reaction [33]. On the other hand, the introduction of carboxyl group in hybrids could break the balance of content between the original epoxy group and curing group, thus decreasing the crosslinking density.

The T_g values of cured CATA-reinforced epoxy resin systems are determined from the peak temperatures of *tan δ vs.* temperature curve; the results are shown in Tab. 3. As shown in Fig. 6(D), the curves of CATA-reinforced epoxy resin systems are similar to those of neat epoxy system and showed only a single peak, indicating that all systems have no traces of phase separation [48]. Compared with neat epoxy system, all the CATA-reinforced epoxy resin system showed a higher T_g. In addition, T_g first increased with increasing CATA loading and then decreased at higher loadings (2.0 wt% and 3.0 wt%). The T_g of CATA 1reached up to the maximum of 159.7°C, 25.2°C higher than neat epoxy system (134.5°C). However, when the CATA loading was high (> 1.0 wt%), the T_g of CATA-reinforced epoxy resin systems decreased slightly. T_g was affected by the chain segment mobility and crosslinking density [49].The increase in T_g can be explained as follows: The rigid inner aromatic core of CATA limits the chain segment mobility and increases the chain rigidity to some degrees. At higher CATA loadings, the T_g of CATA-reinforced epoxy resin systems decreased slightly. This is probably because an excess of CATA was incorporated into neat epoxy system, thus increasing the steric hindrance effect and leading to an incomplete curing reaction. In addition, the flexible backbone of CATA showed dilution effect and led to an additional decrease in T_g [48].

Based on the free volume theory [10], the fractional free volume at temperature $T(f_T)$ can be expressed as follows:

$$f_T = f_g + \Delta\alpha_v (T - T_g) \tag{2}$$

where $\Delta\alpha_v = \alpha_r - \alpha_g$ is the difference between the volumetric coefficients of thermal expansion (CTE) in rubbery region (α_r) and glassy region (α_g), and f_g is the fractional free volume "frozen" at T_g. $\Delta\alpha_v$ can be treated as the fractional free volume, as confirmed by positron annihilation lifetime spectroscopy (PALS) measurements. The CTE in the rubbery state and glassy state as well as Δα are shown in Tab. 4. Compared with neat epoxy system, the glassy region (α_g) of CATA-reinforced epoxy resin systems showed that α_g decreased with the incorporation of CATA. Notably, CATA 1 has the lowest α_g among all other systems, thus maintaining better interfacial strength during shocks and temperature cycles [10,50]. As the CATA loading increased from 0 to 3.0 wt%, α_g showed a systematic decrease, whereas α_r showed a systematic increase. Thus, $\Delta\alpha$ showed a systematic increase, indicating that the introduction of CATA into the epoxy resin system provided more fractional free volume.

Based on the above comprehensive analysis, it can be concluded that the increase in fractional free volume was beneficial to the increase in impact strength and fracture elongation.

Table 4: Linear coefficients of thermal expansion determined from DMA measurements

Sample	α_g(×10^{-6} K^{-1}) [a]	α_r(×10^{-6}K^{-1})[a]	$\Delta\alpha_{v=\Delta}\alpha_r-\alpha_g$(×10^{-6} K^{-1})[a]
Neat	85.2	187.5	102.3
CATA 0.25	83.7	192.9	109.2
CATA 0.5	80.1	195.6	115.5
CATA 1	74.6	198.7	124.1
CATA 2	75.8	203.1	127.3
CATA 3	78.4	197.1	118.7

[a] α_g, α_r, and $\Delta\alpha_v$ refer to the glassy region, rubbery region, and fractional free volume, respectively.

3.4.3 TGA Analysis

TGA is a simple method to evaluate the degradation behavior and thermal stability of polymers. To evaluate the effect of CATA content, the thermal stability of as-prepared CATA-reinforced epoxy resin systems was measured. The results are shown in Tab. 2 and Figs. 7(A) and 7(B). The thermal stability parameters are $T_{5\%}$ (the temperature corresponding to 5% weight loss) and $T_{50\%}$ (the temperature corresponding to 50% weight loss). As shown in Fig. 7(A), clearly the $T_{5\%}$ and $T_{50\%}$ of CATA-reinforced epoxy resin systems decreased slightly with increasing CATA loadings from 0 to 3.0 wt%. This can be attributed to the polyester backbones of TA core. For example, CATA 0.25 and CATA 1 decreased the $T_{5\%}$ from 350.8°C to 295.4°C and the $T_{50\%}$ from 463.5°C to 456.6°C, respectively. In addition, the shapes of DTG curves for two systems are unimodal, indicating that the structure of CATA-reinforced epoxy resin systems is not different from that of neat epoxy system in thermal stability. In general, a small amount of CATA was introduced into epoxy resin systems. Thus, the thermal stability of CATA-reinforced epoxy resin systems was affected, but the result was within an acceptable level.

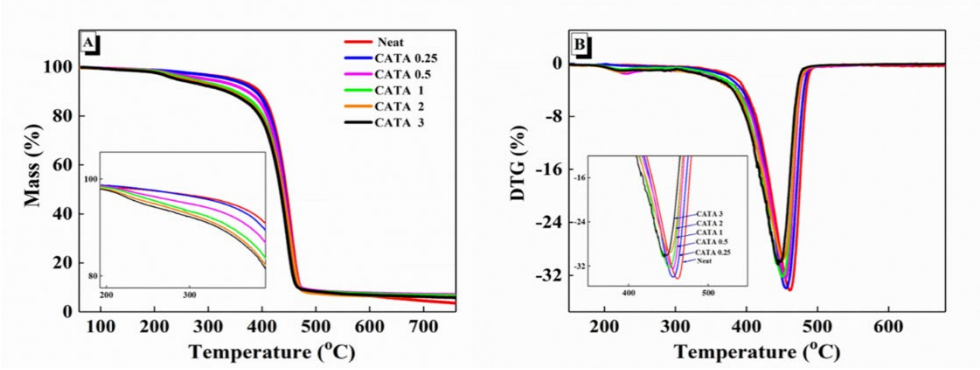

Figure 7: TGA (A) and DTG (B) curves of CATA-reinforced epoxy resin systems with different CATA loadings

4 Conclusions

A high-performance, solvent-free epoxy resin was developed using CATA as a bio-based hyperbranched toughener. The mechanical performance, morphology, structural characterization, and thermal characterization of modified solvent-free epoxy resin systems were studied. At only 1.0 wt% loading, the CATA-reinforced epoxy resin system exhibits a nearly 111% increase in the impact strength (from 7.9 KJ/m^2 to 16.7 KJ/m^2). Notably, the tensile strength and elongation at break of CATA-reinforced epoxy resin systems increased moderately with increasing CATA loadings. The SEM and DMA results show that CATA-reinforced epoxy resin system have no traces of phase separation. Additionally, the SEM and DMA results further confirm that the CATA incorporated into the epoxy resin system improved the toughness as evident from fibril formation. A combination of high strength, high heat resistance, and high toughness for solvent-free epoxy resin is an important factor for their practical applications. This work will allow us to comprehensively understand the mechanical and thermal properties of solvent-free epoxy resins and contribute to fabricating and screening high-performance, solvent-free epoxy resins.

Acknowledgments: We acknowledge the financial support from the Special Fund for the Program for Zhejiang Provincial Natural Science Foundation of China (LZ16C160001), National Key Research and Development Program (2017YFD0601105), the National Natural Science Foundation of China (Grant No. 21806142), and the Zhejiang Provincial Natural Science Foundation of China (Grant No. LY20B070002).

References

1. Fei, X., Wei, W., Zhao, F., Zhu, Y., Luo, J. et al. (2017). Efficient toughening of epoxy-anhydride thermosets with a biobased tannic acid derivative. *ACS Sustainable Chemistry & Engineering, 5(1),* 596-603.
2. Fei, X., Zhao, F., Wei, W., Luo, J., Chen, M. et al. (2016). Tannic acid as a bio-based modifier of epoxy/anhydride thermosets. *Polymers, 8(9),* 314.
3. Sharifi, M., Ebrahimi, M., Jafarifard, S. (2017). Preparation and characterization of a high performance powder coating based on epoxy/clay nanocomposite. *Progress in Organic Coatings,106,* 69-76.
4. Wuzella, G., Kandelbauer, A., Mahendran, A. R., Müller, U., Teischinger, A. (2014). Influence of thermo-analytical and rheological properties of an epoxy powder coating resin on the quality of coatings on medium density fibreboards (MDF) using in-mould technology. *Progress in Organic Coatings, 77(10),* 1539-1546.
5. Yu, H., Wang, L., Shi, Q., Jiang, G., Zhao, Z. et al. (2006). Study on nano-$CaCO_3$ modified epoxy powder coatings. *Progress in Organic Coatings, 55(3),* 296-300.
6. Mafi, R., Mirabedini, S., Attar, M., Moradian, S. (2005). Cure characterization of epoxy and polyester clear powder coatings using differential scanning calorimetry (DSC) and dynamic mechanical thermal analysis (DMTA). *Progress in Organic Coatings, 54(3),* 164-169.
7. Kozakiewicz, J., Ofat, I., Legocka, I., Trzaskowska, J. (2014). Silicone-acrylic hybrid aqueous dispersions of core-shell particle structure and corresponding silicone-acrylic nanopowders designed for modification of powder coatings and plastics. Part I-Effect of silicone resin composition on properties of dispersions and corresponding nanopowders. *Progress in Organic Coatings, 77(3),* 568-578.
8. Ren, W., Pan, X., Wang, G., Cheng, W., Liu, Y. (2016). Dodecylated lignin-g-PLA for effective toughening of PLA. *Green Chemistry, 18(18),* 5008-5014.
9. Auvergne, R., Caillol, S., David, G., Boutevin, B., Pascault, J. P. (2014). Biobased thermosetting epoxy: present and future. *Chemical Reviews,114(2),* 1082-1115.
10. Liu, T., Nie, Y., Chen, R., Zhang, L., Meng, Y. et al. (2015). Hyperbranched polyether as an all-purpose epoxy modifier: controlled synthesis and toughening mechanisms. *Journal of Materials Chemistry A, 3(3),* 1188-1198.
11. Wang, K., Chen, L., Wu, J., Toh, M. L., He, C. et al. (2005). Epoxy nanocomposites with highly exfoliated clay: mechanical properties and fracture mechanisms. *Macromolecules, 38(3),* 788-800.
12. Wang, R., Zhuo, D., Weng, Z., Wu, L., Cheng, X. et al. (2015). A novel nanosilica/graphene oxide hybrid and its flame retarding epoxy resin with simultaneously improved mechanical, thermal conductivity, and dielectric properties. *Journal of Materials Chemistry A, 3(18),* 9826-9836.
13. Ma, Q., Luo, J., Chen, Y., Wei, W., Liu, R. et al. (2015). Reactive copolymer functionalized graphene sheet for enhanced mechanical and thermal properties of epoxy composites. *Journal of Polymer Science Part A: Polymer Chemistry, 53(23),* 2776-2785.
14. Ding, C., Matharu, A. S. (2014). Recent developments on biobased curing agents: a review of their preparation and use. *ACS Sustainable Chemistry & Engineering, 2(10),* 2217-2236.
15. Cao, L., Liu, X., Na, H., Wu, Y., Zheng, W. et al. (2013). How a bio-based epoxy monomer enhanced the properties of diglycidyl ether of bisphenol A (DGEBA)/graphene composites. *Journal of Materials Chemistry A, 1(16),* 5081-5088.
16. El Mansouri, N. E., Yuan, Q., Huang, F. (2011). Characterization of alkaline lignins for use in penol-formaldehyde and epoxy resins. *Bioresources, 6(3),* 2647-2662.
17. Yang, G., Rohde, B. J., Tesefay, H., Robertson, M. L. (2016). Biorenewable epoxy resins derived from plant-based phenolic acids. *ACS Sustainable Chemistry & Engineering, 4(12),* 6524-6533.
18. Liu, X., Zong, E., Hu, W., Song, P., Wang, J. et al. (2019). Lignin-derived porous carbon loaded with La(OH)3 nanorods for highly efficient removal of phosphate. *ACS Sustainable Chemistry & Engineering, 7(1),* 758-768.
19. Zong, E., Liu, X., Jiang, J., Fu, S., Chu, F. (2016). Preparation and characterization of zirconia-loaded lignocellulosic butanol residue as a biosorbent for phosphate removal from aqueous solution. *Applied Surface Science, 387,* 419-430.
20. Zong, E., Huang, G., Liu, X., Lei, W., Jiang, S. et al. (2018). A lignin-based nano-adsorbent for superfast and highly selective removal of phosphate. *Journal of Materials Chemistry A, 6(21),* 9971-9983.

21. Zong, E., Liu, X., Liu, L., Wang, J., Song, P. et al. (2018). Graft polymerization of acrylic monomers onto lignin with $CaCl_2$-H_2O_2 as initiator: preparation, mechanism, characterization, and application in poly(lactic acid). *ACS Sustainable Chemistry & Engineering, 6(1),* 337-348.
22. Qiao, X., Zhao, C., Shao, Q., Hassan, M. (2018). Structural characterization of corn stover lignin after hydrogen peroxide presoaking prior to ammonia fiber expansion pretreatment. *Energy & Fuels, 32(5),* 6022-6030.
23. Yu, J., Lu, C., Wang, C., Wang, J., Fan, Y. et al. (2017). Sustainable thermoplastic elastomers derived from cellulose, fatty acid and furfural via ATRP and click chemistry. *Carbohydrate Polymers, 176,* 83-90.
24. Yu, J., Zhu, Y., Ma, H., Liu, L., Hu, Y. et al. (2019). Contribution of hemicellulose to cellulose nanofiber-based nanocomposite films with enhanced strength, flexibility and UV-blocking properties. *Cellulose, 26(10),* 6023-6034.
25. Ma, Q., Liu, X., Zhang, R., Zhu, J., Jiang, Y. (2013). Synthesis and properties of full bio-based thermosetting resins from rosin acid and soybean oil: the role of rosin acid derivatives. *Green Chemistry, 15(5),* 1300-1310.
26. Nouailhas, H., Aouf, C., Le Guerneve, C., Caillol, S., Boutevin, B. et al. (2011). Synthesis and properties of biobased epoxy resins. Part 1. Glycidylation of flavonoids by epichlorohydrin. *Journal of Polymer Science Part A: Polymer Chemistry, 49(10),* 2261-2270.
27. Huang, K., Liu, Z., Zhang, J., Li, S., Li, M. et al. (2014). Epoxy monomers derived from tung oil fatty acids and its regulable thermosets cured in two synergistic ways. *Biomacromolecules, 15(3),* 837-843.
28. Jia, P., Hu, L., Zhang, M., Feng, G., Zhou, Y. (2017). Phosphorus containing castor oil based derivatives: Potential non-migratory flame retardant plasticizer. *European Polymer Journal, 87,* 209-220.
29. Jia, P., Zhang, M., Hu, L., Feng, G., Bo, C. et al. (2015). Synthesis and application of environmental castor oil based polyol ester plasticizers for poly(vinyl chloride). *ACS Sustainable Chemistry & Engineering, 3(9),* 2187-2193.
30. Pan, X., Sengupta, P., Webster, D. C. (2011). Novel biobased epoxy compounds: epoxidized sucrose esters of fatty acids. *Green Chemistry, 13(4),* 965-975.
31. Ma, S., Liu, X., Fan, L., Jiang, Y., Cao, L. et al. (2014). Synthesis and properties of a bio-based epoxy resin with high epoxy value and low viscosity. *ChemSusChem, 7(2),* 555-562.
32. Kristufek, S. L., Yang, G., Link, L. A., Rohde, B. J., Robertson, M. L. et al. (2016). Synthesis, characterization, and cross-linking strategy of a quercetin-based epoxidized monomer as a naturally-derived replacement for BPA in epoxy resins. *ChemSusChem, 9(16),* 2135-2142.
33. Liu, X., Wang, J., Li, S., Zhuang, X., Xu, Y. et al. (2014). Preparation and properties of UV-absorbent lignin graft copolymer films from lignocellulosic butanol residue. *Industrial Crops and Products, 52,* 633-641.
34. Boro, U., Karak, N. (2017). Tannic acid based hyperbranched epoxy/reduced graphene oxide nanocomposites as surface coating materials. *Progress in Organic Coatings, 104,* 180-187.
35. Deng, Y., Feng, X., Zhou, M., Qian, Y., Yu, H. et al. (2011). Investigation of aggregation and assembly of alkali lignin using iodine as a probe. *Biomacromolecules, 12(4),* 1116-1125.
36. Thielemans, W., Wool, R. P. (2005). Lignin esters for use in unsaturated thermosets: lignin modification and solubility modeling. *Biomacromolecules, 6(4),* 1895-1905.
37. Arbenz, A., Avérous, L. (2015). Chemical modification of tannins to elaborate aromatic biobased macromolecular architectures. *Green Chemistry, 17(5),* 2626-2646.
38. Liu, X., Xin, W., Zhang, J. (2009). Rosin-based acid anhydrides as alternatives to petrochemical curing agents. *Green Chemistry, 11(7),* 1018-1025.
39. Gandini, A. (2008). Polymers from renewable resources: a challenge for the future of macromolecular materials. *Macromolecules, 41(24),* 9491-9504.
40. Wang, J., Yu, J., Liu, Y., Chen, Y., Wang, C. et al. (2013). Synthesis and characterization of a novel rosin-based monomer: free-radical polymerization and epoxy curing. *Green Materials, 1(2),* 105-113.
41. Bagheri, R., Marouf, B., Pearson, R. (2009). Rubber-toughened epoxies: a critical review. *Journal of Macromolecular Science®, Part C: Polymer Reviews, 49(3),* 201-225.
42. Xu, J., Yang, J., Liu, X., Wang, H., Zhang, J. et al. (2018). Preparation and characterization of fast-curing powder epoxy adhesive at middle temperature. *Royal Society Open Science, 5(8),* 180566.

43. Huang, D. D., Xu, F., Du, X. S., Lee, Z. H., Wang, X. J. (2017). Temperature effects on rigid nano-silica and soft nano-rubber toughening in epoxy under impact loading. *Journal of Applied Polymer Science, 134(38),* 45319.
44. Lv, J., Meng, Y., He, L., Qiu, T., Li, X. et al. (2013). Novel epoxidized hyperbranched poly (phenylene oxide): synthesis and application as a modifier for diglycidyl ether of bisphenol A. *Journal of Applied Polymer Science, 128(1),* 907-914.
45. Liu, Y., Ramirez, C., Zhang, L., Wu, W., Padture, N. P. (2017). In situ direct observation of toughening in isotropic nanocomposites of alumina ceramic and multiwall carbon nanotubes. *Acta Materialia, 127,* 203-210.
46. Zhang, Z., Zhang, Y., Lin, Z., Mulyadi, A., Mu, W. et al. (2017). Butyric anhydride modified lignin and its oil-water interfacial properties. *Chemical Engineering Science, 165,* 55-64.
47. Luo, L., Meng, Y., Qiu, T., Li, X. (2013). An epoxy-ended hyperbranched polymer as a new modifier for toughening and reinforcing in epoxy resin. *Journal of Applied Polymer Science, 130(2),* 1064-1073.
48. Liu, T., Nie, Y., Zhang, L., Chen, R., Meng, Y. et al. (2015). Dependence of epoxy toughness on the backbone structure of hyperbranched polyether modifiers. *RSC Advances, 5(5),* 3408-3416.
49. Kaji, M., Nakahara, K., Endo, T. (1999). Synthesis of a bifunctional epoxy monomer containing biphenyl moiety and properties of its cured polymer with phenol novolac. *Journal of Applied Polymer Science, 74(3),* 690-698.
50. Huang, X., Roth, C. B. (2018). Optimizing the grafting density of tethered chains to alter the local glass transition temperature of polystyrene near silica substrates: the advantage of mushrooms over brushes. *ACS Macro Letters, 7(2),* 269-274.